

## PHASE TRANSFORMATION AND MICROSTRUCTURE IN Nb-V ALLOYED C-Mn STEEL

Dr.Eng. R. Petrov, Prof.Dr.Ir. L. Kestens, and Prof.Dr. Ir.Y. Houbaert

Department of Metallurgy and Materials Science, Ghent University, Ghent, Belgium.

*A Continuous Cooling Transformation (CCT) diagram of a 0.082%C, 1.54% Mn, 0.35% Si, 0.055%Nb and 0.078%V steel was experimentally determined by means of dilatometry test, metallography and hardness measurements. The austenite non-recrystallization temperature and the position of the Ar<sub>3</sub> temperature were determined by means of hot torsion simulation of the rolling schedule. The validity of the CCT diagram was experimentally confirmed by means of controlled rolling experiments followed by quenching in order to quantify the intercritical ferrite volume fraction. These data could be used for the design of rolling schedules for controlled rolling of thin strips with fine grains an appropriate texture.*

### Introduction

In contemporary line pipe technologies both strength and toughness of the steel are of great importance. This combination of properties could be achieved by changing the chemical composition of the steel or by proper thermo-mechanical processing (TMP) that both contribute to a development of fine-grained microstructure and appropriate texture in the hot rolled plate.

The influence of the different type of transformation textures on the anisotropy of tensile strength are summarised by Ray and Jonas [1]. In a later work Baczinsky *et. al* [2] have analysed the influence of the microstructure and texture on the toughness of high strength steels for the pipelines that were finish rolled either above or below the Ar<sub>3</sub> temperature. In both cases the authors observe the positive influence of the texture components in the vicinity of the ND fiber ( $\langle 111 \rangle // ND$ ) on the plastic anisotropy and toughness.

In some cases, like rolling of thin gauge strips, the steel manufacturers finish the rolling in the intercritical  $\gamma+\alpha$  region. It was reported elsewhere [3, 4, 5, 6] that intercritical rolling gives rise to an undesirable coarse-grained microstructure and a texture gradient from the surface to the center of the strips [4]. Vanderschueren *et al* [4] studied the microstructure and texture in a number of industrially hot rolled plain carbon steels and Ti added steels by means of XRD texture measurements. They observe large ferrite grains in plain carbon steel strips after finish rolling in  $\gamma+\alpha$  region, together with unwanted transformation texture components. They explain this behaviour by the existence of austenite grains that transform to dislocations free ferrite grains, which will act as nuclei for the subsequent recrystallization of the strained ferrite. The authors have named this phenomenon *transformation induced recrystallization* and mention that it does not appear when Ti based precipitates interact with the recrystallization. The same explanation is given by Bodin *et al* [5, 6] for the observed ferritic

grain growth after intercritical rolling of C-Mn and low carbon steels.

Just the opposite effect of strong grain refinement is observed by Bleck *et al* [7] after uniaxial compression of a C-Mn-Nb steel in the intercritical region followed by controlled cooling, in order to avoid a bainite and martensite transformation. A similar effect together with a specific distribution of the transformation texture components among the different sized ferrite grains in Nb micro alloyed steel and a favourable deep drawing texture in plain carbon steels were observed by Petrov *et al* [8] in industrially rolled thin gauge strips. They associate the changes in the transformation texture and grain size with the amount of strain in the austenite region at different temperatures.

Therefore, the reason for these two contradictive opinions about the influence of intercritical rolling on the microstructure might be related to the chemical composition of the steel or to the exact control of the thermo mechanical processing parameters. When the thermo-mechanical parameters are suitably set for the chemical composition of the steel, it seems to be possible to obtain a very good combination of fine grains and appropriate texture that will lead to a high strength, improved toughness and low mechanical anisotropy. In the opposite case, however, with an inappropriate control of thermo-mechanical parameters, large grains and unfavourable textures are obtained (e.g. a very strong  $\{001\} \langle 110 \rangle$  component), which cause a drastic decrease in toughness and a strong mechanical anisotropy. Hence, the accurate control of the thermo-mechanical processing parameters is of key importance for the quality of the final product, and it is possible to be carried out if and only if the transformation characteristics of the steel are accurately determined. It is not enough only to know the CCT diagram of the steel because the CCT diagrams describe the transformation in non-strained austenite, although the Ar<sub>3</sub> temperatures of strained and non-strained austenite differ significantly. The Ar<sub>3</sub> temperature of strained austenite is shifted to higher values, which increases the probability that the final

rolling pass is carried out in the intercritical temperature region.

The goal of the present work is to obtain a better understanding of the  $\gamma$ - $\alpha$  phase transformation of a Nb-V-alloyed C-Mn steel in strained and unstrained conditions in order to use this data for further accurate design of the thermo-mechanical processing schedules.

### Experimental

The chemical composition of the steel, which was used in this work was determined by means of optical emission spectrometry on the "Spectrolab®" equipment and the results are shown in table 1 (in mass content in %). Table 1

Chemical composition, mass. %									
C	Mn	P	S	Si	Al	Nb	V	N	
0.082	1.54	0.01	0.006	0.36	0.033	0.055	0.078	0.005	

In order to determine the occurrence of inhomogeneities of the chemical composition caused by segregation of the substitutional elements a local EDX mapping of Mn and Si was applied on the cross section of the steel plates.

Cylindrical samples with 5 mm length and 3.5 mm diameter were cut out of the central part of the steel plate and they were used in a Tetha Dilatronic IIS quench dilatometer to study the phase transformation of the steel in non-strained conditions. The samples were reheated by an induction coil in vacuum at a constant reheating rate of 10°C/s to 1200°C and kept for 2 min for complete homogenisation and next cooling down with constant cooling rates, which varied from 10 to 4000°C/min. The dilatometry tests in combination with metallographic

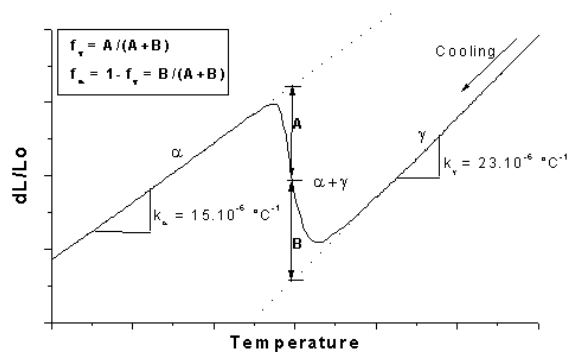


Fig. 1 A schematic presentation of the "lever rule" used to determine the volume fraction  $f_\alpha$  and  $f_\gamma$  of the phases during  $\alpha$  to  $\gamma$  phase transformation. The linear thermal expansion coefficients of the phases are  $k_\alpha$  and  $k_\gamma$ , respectively.

examination and hardness tests allow to determine the CCT diagram of the steel for the case when the austenite phase is not strained prior to transformation. The "lever rule" was used for quantification of the transformed phases as it is shown in Fig.1 [9].

The austenite non-recrystallization temperature ( $T_{nr}$ ) as well as the  $A_{r3}$  temperature of the strained austenite ( $A_{r3}^d$ ) were determined by simulating the hot rolling process on a hot torsion device, according to the method proposed by Maccagno et al [10].

The hot rolling was carried out in a reversible hot rolling mill. The temperature during the rolling was controlled by means of K1 type thermocouples that were embedded in the rolled sheet as well as by two pyrometers installed on the rolling mill. This approach allows to compare the results that were obtained by DSC or torsion test with ones obtained on the rolling mill.

Optical microstructural analyses together with orientation image analyses (OIM) were used for qualitative and quantitative analyses of the samples after hot rolling. A number of OIM assessments was also carried out on the samples that were used for DSC characterization.

### Results and discussion

Fig. 1 displays an example of the EDX mapping of the Mn and Si in the as-received material. The upper line, marked with squares, shows the distribution of Mn and the lower line, marked with diamonds, represents the Si distribution.

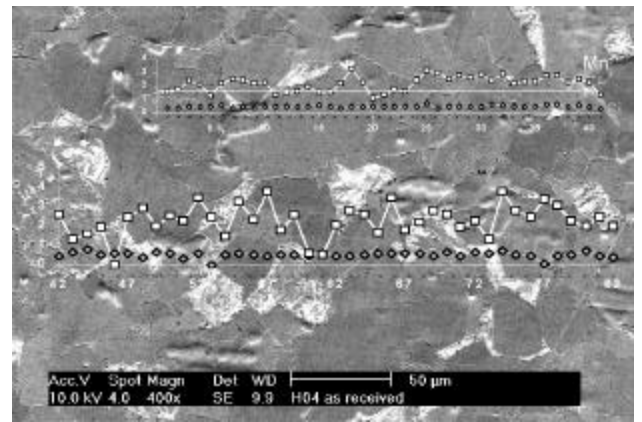


Fig.2 Distribution of Mn and Si in the as received rough rolled blocks.

The dilatometer curves are shown in fig. 3 to fig. 6, together with the recalculated curves of the transformed volume fraction of the different phases. The temperature which corresponds to 5% and 95% of transformed volume fraction was considered to mark the start and end of the phase transformation, respectively. This approach allows to minimise the inaccuracies on the determination of the

phase transformation start and end temperatures. Fig. 3a displays the transformation behaviour of the steel during reheating to 1200°C at 10°C/s and the transformed volume fraction is shown in fig. 3b. In fig. 4a the changes of dilatation vs. temperature are shown for a number of samples cooled down with rates from 10 to 4000°C/min, whereas the transformed volume fraction of the same is shown in Fig. 4b.

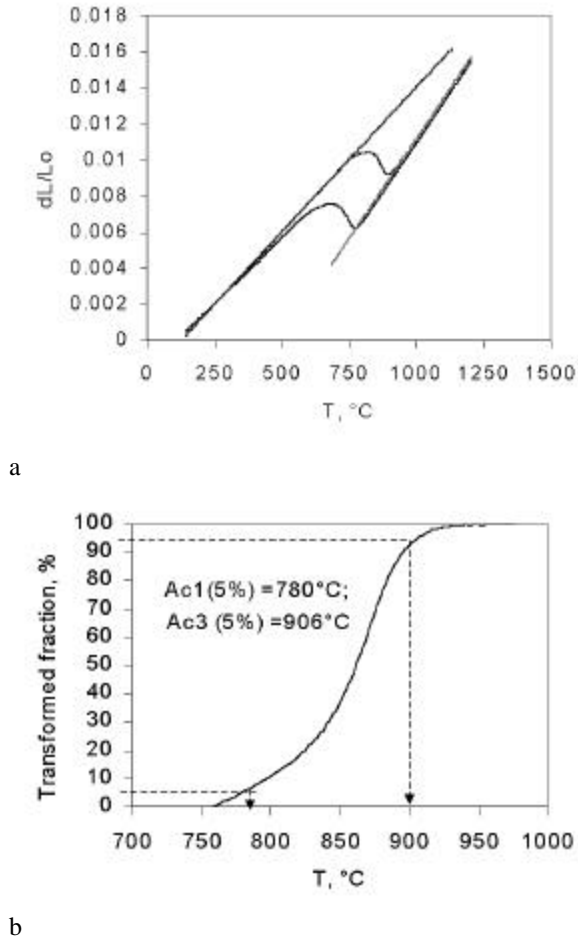


Fig.3 (a) A dilatometer record obtained during reheating at 10°C/s to 1200°C and cooling down at 10°C/min. The straight lines indicated calculated values of the thermal expansion of  $\alpha$  and  $\gamma$  phases.; (b) Calculated curve, which displays the transformed  $\gamma$  fraction as a function of reheating temperature.

For the cooling rates higher than 10°C/min one observes changes in the slope of the *transformed fraction vs. temperature* curve. These inflection points were used to determine the onset of pearlite or bainite start temperature in a combination with the microstructural studies. From the microstructures, shown in fig.5, it is evident that after cooling at cooling rates higher than 20°C/min a significant part of the microstructure transforms to bainite and at 300°C/min the amount of ferrite is restricted to ~7-8% mainly in the former

austenite grain boundaries. For this reheating and cooling conditions the average austenite grain size was determined to be ~200  $\mu m$ .

These data allow to determine the continues cooling transformation (CCT) diagram for the steel. It should be mentioned that if the diagram is constructed only on the base of these data, it would not give a correct description of the transformation behaviour of the material because the CCT diagram does not take into account the fact that during thermo-mechanical treatment the  $\gamma$ - $\alpha$  transformation starts in strained austenite matrix, which could introduce a significant shift of the position of  $Ar_3$  temperatures toward higher values.

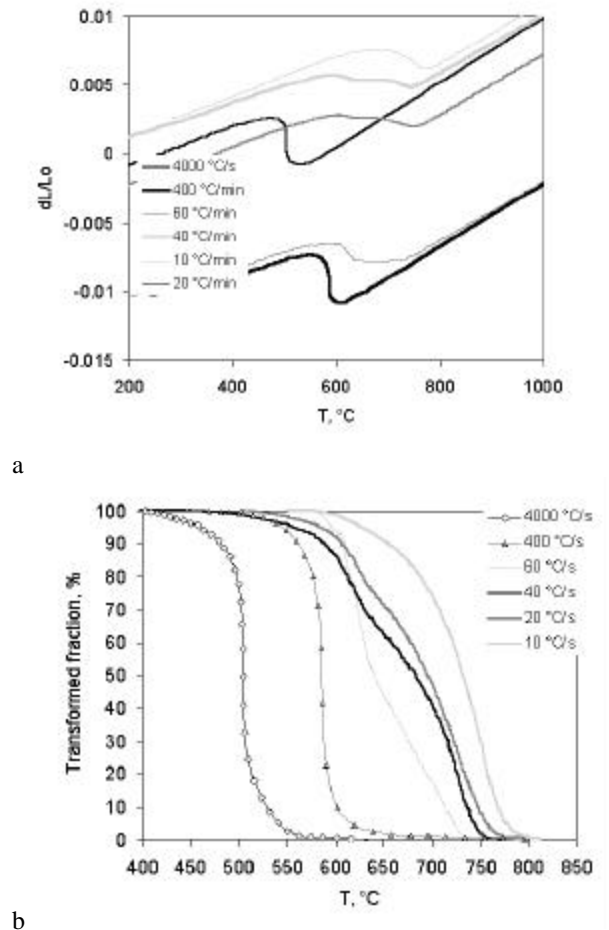


Fig.4. (a) Dilatometry records of the transformation observed during cooling to room temperature at various cooling rates varying from 10 to 4000°C/min and (b) corresponding plots of the transformed volume fraction vs. temperature.

The exact position of  $Ar_3$  of strained austenite, denominated from hereon  $Ar_3^d$ , is of key importance for controlled rolling because it separates the austenite from the two-phase  $\gamma+\alpha$  region. The  $Ar_3^d$  temperatures together with the  $T_{nr}$  (austenite non-recrystallization temperature) are determined by hot torsion simulations. By definition

the non-recrystallization temperature of austenite, is the temperature below which the strained austenite does not recrystallize entirely any more and a fine pancaked structure is produced. The  $T_{nr}$  temperature could be determined experimentally but can also be calculated by employing the following formula proposed by *Borrato et al*[11].

$$T_{nr} = 887 + 464C + 890Ti + 363Al - 357Si + 6445Nb - 644\sqrt{Nb} + 732V - 230\sqrt{V}$$

(1)

The calculated value of  $T_{nr}$  was found to be 1024°C.

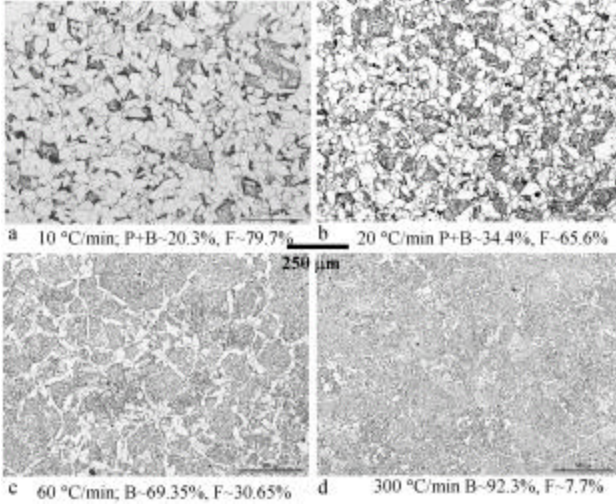


Fig. 5. a-d Microstructures of the steel observed after cooling with different cooling rates from 1200°C. The volume fraction of the different structural elements is mentioned on the photos (P = pearlite, B = bainite, F = ferrite).

Table 2

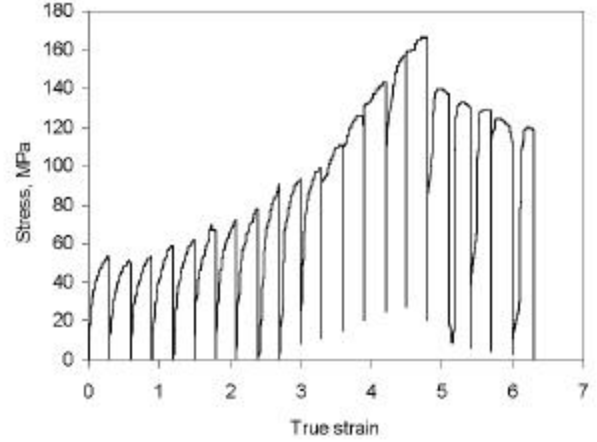
1	T, °C	Time, min	First pass at °C	$\dot{\epsilon}$	$\dot{\gamma}$ , s <sup>-1</sup>	Cooling rate, °C/s	Inter-pass time, s	$T_{nr}$ °C	$Ar_3^d$ °C
1	1200	5	1200	0.3	5	1	30	1050	835
2	1200	5	1200	0.3	1	1	30	1074	810
3	1250	2	1150	0.3	1	1	15	1025	800
4	1200	2	1150	0.3	1	1	10	1023	770
5	1200	2	1150	0.3	1	6.8	10	-	730

Hot torsion tests were performed in order to simulate the hot rolling and determine the actual  $T_{nr}$  temperature. Cylindrical samples with 6 mm diameter were reheated to 1200°C, twisted at a strain rate of 1 s<sup>-1</sup> with a strain of 0.3 in each pass at interval temperatures of 20 °C during cooling at a rate of 60, 240, 360 and 600 °C/min, and with an interpass time of 10 s. Fig.6a shows the effective stress-effective strain curves and fig.6b displays the recalculated *mean flow stress vs. temperature* obtained at a cooling rate of 60°C/min. The mean flow stress (MFS) is the area under each  $\sigma$ - $\epsilon$  curve divided by

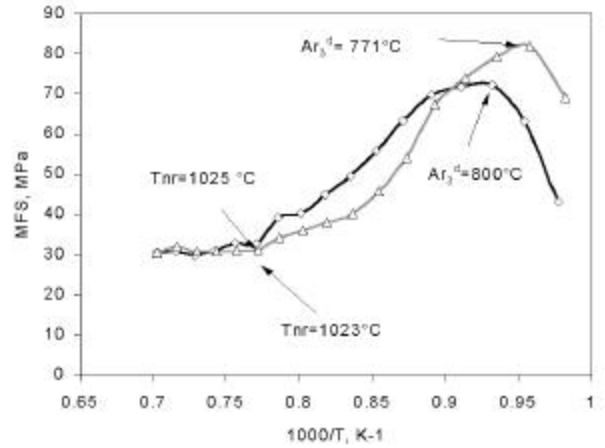
the total deformation. It is defined by the following equation:

$$MFS = \frac{1}{e_b - e_a} \int_a^b \sigma de \quad (2)$$

Some important testing parameters are given in Table 2.



a



b

Fig.6. (a) Data from torsion test regime 3 (cf. table 2) and (b) recalculated mean flow stress plotted versus the 1000/T for the regimes 3 and 4 (table 2).

$T_{nr}$  was determined by the change in the slope of the MFS-1000/T curve and  $Ar_3$  at the point where the MFS starts to decrease. The averaged data calculated on the basis of at least 3 measurements are shown in Fig.6 b.

Based on the dilatometry and torsion data, the CCT diagram of the steel for strained and not strained pre-transformation conditions of the  $\gamma$  phase was designed. The diagram is shown in fig.7 and table 3 lists the critical temperatures obtained in the present work together with the calculated values of these temperatures by means of the existing models.

The additional small squares connected with a dotted line display the position of  $Ar_3^d$  temperature

determined by means of hot torsion. The applied deformation shifts the temperatures of the  $\gamma$ - $\alpha$  transformation to higher values ( $\sim 50^\circ\text{C}$ ) with respect to their value in non-strained condition. The cooling rates marked by dotted lines correspond to the experimentally measured ones in the middle thickness of the strips during the controlled rolling. They vary between 260 and  $700^\circ\text{C}/\text{min}$  as a function of the rolling parameters. The combination of both factors — cooling rate of the rolling mill and the position of  $\text{Ar}_3^d$  temperature allows to determine the processing window for intercritical rolling, which is extended to elevated temperatures, with respect to the conventional CCT diagram as it is shown in Fig.7 (hatched zone).

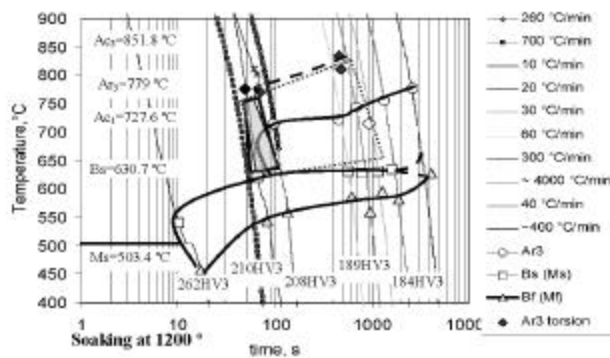


Fig.7. Experimentally deduced CCT diagram together with the position of the  $\text{Ar}_3^d$  temperature.

Table3

Temperature	Calculated	Measured	References
$\text{Ac}_1$	727.6	780 ( $5^\circ\text{C}/\text{s}$ )	Andrews [12]
$\text{Ac}_3$	851	906 ( $5^\circ\text{C}/\text{s}$ )	Andrews [12]
$\text{Ar}_3$	779	776	Kestens & Vanderschueren [4]
$\text{B}_s$	630.7	626-636	Stevens & Hayns [13]
$\text{M}_s$	503.4	510	Kung & Raymond [14]

Based on these data different rolling schedules were carried out with a final rolling temperatures above the  $\text{Ar}_3^d$  temperature followed by water quenching at different temperatures of the intercritical region. The microstructure measurements displayed that the CCT diagram with the extended position of the  $\text{Ar}_3^d$  temperature gives very accurate prediction of the phase transformation in the processing conditions of austenite during hot rolling.

Fig 8 a and b display an example taken from the microstructure of samples that were hot rolled both with final rolling pass in the austenite region at  $850^\circ\text{C}$  and afterwards water quenched at a temperature of  $800^\circ\text{C}$ (fig.8a) and  $720^\circ\text{C}$  (fig.8b), respectively. When the

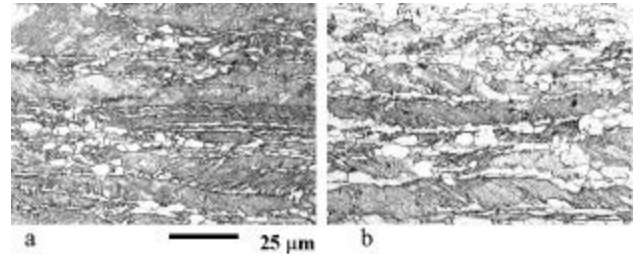


Fig.8 Microstructures of the samples those were finish rolled at  $850^\circ\text{C}$  and quenched (a) at  $800^\circ\text{C}$  and (b) at  $720^\circ\text{C}$ .

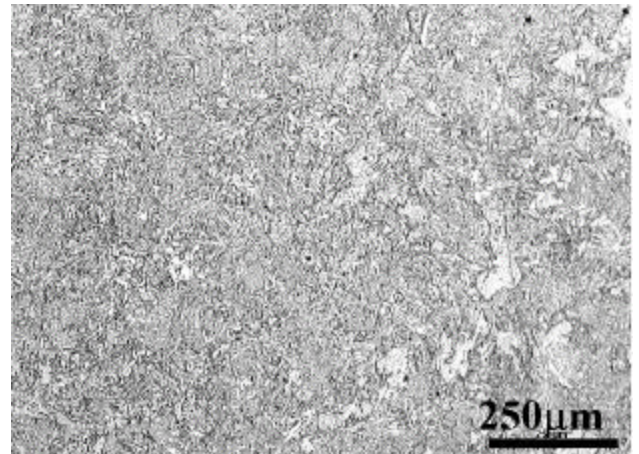


Fig.9 Microstructure of the non-deformed samples cooled to  $780^\circ\text{C}$  at  $400^\circ\text{C}$  and next water quenched

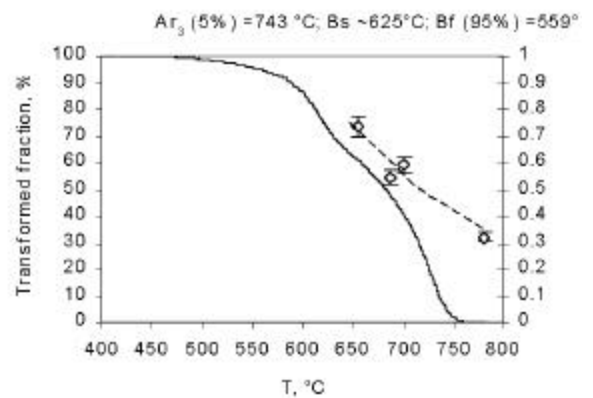


Fig. 10. Quantification of ferrite volume fraction in non-deformed (solid line) and deformed samples prior to the transformation (dotted line)

austenite phase is not strained prior to the  $\gamma$ - $\alpha$  transformation the microstructure after water quenching from  $780^\circ\text{C}$  is a homogeneous martensite (fig.9). The ferrite volume fraction was quantified and plotted as a

function of the (intercritical) quench temperature together with the transformation curve for non-strained austenite obtained with the same cooling rate of 300°C/min (fig.10).

### Conclusions

A Continuous Cooling Transformation (CCT) diagram of a 0.082%C, 1.54% Mn, 0.35% Si, 0.055%Nb and 0.078%V steel was experimentally determined by means of dilatometry test, metallography and hardness measurements. The experimental results are in very good agreement with the theoretical predicted values. The austenite non-recrystallization temperature and the position of the  $A_{r3}$  temperature were determined by means of hot torsion simulation of the rolling schedule. The shift of  $A_{r3}^d$  temperature towards the higher temperature region is dependent on the strain and strain rate as well as on the cooling rate during torsion simulation. The validity of the CCT diagram was experimentally approved by means of controlled rolling experiments followed by water quenching in order to quantify the intercritical ferrite volume fraction. These data could be used for designing of rolling schedules for controlled rolling of thin strips in order to obtain fine grains and an appropriate crystallographic texture.

### Acknowledgements:

The authors are gratefully acknowledging the financial support of this study under the NIMR project MC 5.01109 and the RD-CORUS Group for providing the material.

### References

- [1] R.K. Ray and J. J. Jonas, "Transformation Texture in Steels", International Materials Reviews, Vol.35, No4, 1990, 1-35.
- [2] G.J. Baczynski, J.J.Jonas and L.E. Collins, "The Influence of Rolling Practice on Notch Toughness and Texture Development in High Strength Linepipe" Mater. Trans. A, Vol.30A, December, 1999, 3045 – 3054.
- [3] G. Kim and O.Kwon, "Formation of Abnormally Coarse Grain Structure in Hot Rolled Strips" Proc. Thermec 88, ed. by Tamura I., ISIJ, Tokyo, 1988, 668–675.
- [4] D. Vanderschueren, L. Kestens, P.Van Houte, E. Aernoudt, J. Dilewijns, U.Meers, "Influence of Transformation induced Recrystallization on Hot Rolling Textures of Low Carbon Steel Sheet", Mater.Sci and Technology, Vol. 6, 1990, 1247–1259.
- [5] A.Bodin, J.Sietsma and S. Van der Zwaag, "Texture and Microstructure Development during Intercritical Rolling of Low-Carbon Steels", Mater. Trans. A Vol.33, No 6, 2002, 1589 – 1603.
- [6] A.Bodin, J.Sietsma and S. Van der Zwaag, "On the Nature of the Bimodal Grain Size Distribution after Intercritical Deformation of a Carbon –Manganese Steel", Mater. Characterization, Vol. 47, 2002 1589 – 1603.
- [7] W. Bleck, C. Herzig and U. Lorenz, "A Method of Producing Very Fine Ferrite Grains by Means of Hot Forming", Steel Research, Vol. 72, No 10, 2001, 406-41.
- [8] R. Petrov, L. Kestens, P. C. Zambrano, M. P. Guerrero, R. Colás, and Y. Houbaert, "Microtexture of Thin Gauge Hot Rolled Steel Strip", ISIJ International, Vol.43, N° 3 2003, 378-385.
- [9] Melspont C., "Phase Transformations and Microstructure-Mechanical Properties Relations in Complex Phase High Strength Steels" Ph.D. Thesis, Department of Materials Science and Metallurgy, Ghent University, 2002.p.53.
- [10] T.M.Maccagno, J.J.Jonas, S.Yue, B.J.McCrady, R. Slobodan and D. Deeks, 'Determination of Recrystallization Stop Temperature from Rolling Mill Logs and Comparison with Laboratory Simulation Results", ISIJ Int, Vol. 34, N°11, 1994, 917 – 922.
- [11] F. Boratto, R. Barbosa, S. Yue and J.J. Jonas: Proc. Int. Conf. Physical Metallurgy of Thermomechanical Processing of Steels and Other Metals (THERMEC '88), 1988, p.383; ed. I. Tamura, ISIJ, Tokyo.
- [12] K.W. Andrews: JISI, Vol. 203, 1965, p.721.
- [13] W. Stevens and A.G. Haynes, J. of the Iron and Steel Institute, 183, 1956, p. 349
- [14] C.Y. Kung, J.J.Rayment: Metall. Trans. A, 1982, vol. 13A, p.328.